

## Ruthenium-Catalyzed Selective Hydroboronolysis of Ethers

Akash Kaithal, Deepti Kalsi, Varadhan Krishnakumar, Sandip Pattanaik, Alexis Bordet, Walter Leitner, and Chidambaram Gunanathan\*

Cite This: *ACS Catal.* 2020, 10, 14390–14397

Read Online

ACCESS |



Metrics &amp; More



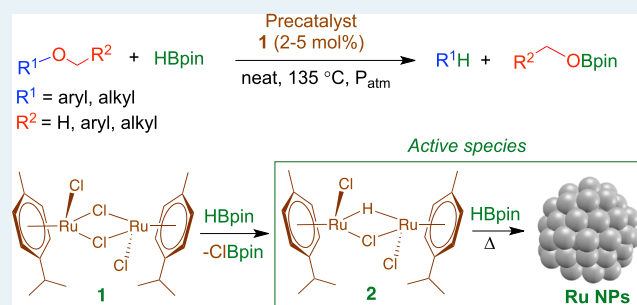
Article Recommendations



Supporting Information

**ABSTRACT:** A ruthenium-catalyzed reaction of HBpin with substituted organic ethers leads to the activation of C–O bonds, resulting in the formation of alkanes and boronate esters via hydroboronolysis. A ruthenium precatalyst, [Ru(*p*-cymene)Cl]<sub>2</sub>Cl<sub>2</sub> (**1**), is employed, and the reactions proceed under neat conditions at 135 °C and atmospheric pressure (ca. 1.5 bar at 135 °C). Unsymmetrical dibenzyl ethers undergo selective hydroboronolysis on relatively electron-poor C–O bonds. In arylbenzyl or alkylbenzyl ethers, C–O bond cleavage occurs selectively on C<sub>Bn</sub>–OR bonds (Bn = benzyl); in alkylmethyl ethers, selective deconstruction of C<sub>Me</sub>–OR bonds leads to the formation of alkylboronate esters and methane. Cyclic ethers are also amenable to catalytic hydroboronolysis. Mechanistic studies indicated the immediate in situ formation of a mono-hydrido-bridged dinuclear ruthenium complex [({η<sup>6</sup>-*p*-cymene)RuCl]<sub>2</sub>(μ-H–μ-Cl)] (**2**), which is highly active for hydroboronolysis of ethers. Over time, the dinuclear species decompose to produce ruthenium nanoparticles that are also active for this transformation. Using this catalytic system, hydroboronolysis could be applied effectively to a very large scope of ethers, demonstrating its great potential to cleave C–O bonds in ethers as an alternative to traditional hydrogenolysis.

**KEYWORDS:** hydroboration, catalysis, hydroelementation, ethers, ruthenium



## INTRODUCTION

The catalytic reductive cleavage of C–O bonds in ethers is a key transformation for the production of fuels and value-added chemicals from biomass.<sup>1–3</sup> In particular, alkyl aryl ether motifs are abundant in lignocellulosic biomass but possess a relatively unreactive C<sub>aryl/alkyl</sub>–O bond.<sup>4–7</sup> The development of catalytic methods allowing their facile deconstruction is thus essential for the valorization of biomass-derived feedstock.<sup>1–3</sup>

In this context, catalytic hydrogenolysis is the most common approach to achieve C–O bond cleavage in ethers.<sup>8</sup> However, other than the palladium-catalyzed hydrogenolysis of benzyl ethers,<sup>9</sup> hydrogenolysis generally requires elevated temperatures, pressures, and specialized equipment. The deconstruction of ethers by conventional synthetic methods requires harsh reaction conditions, including the use of strong acids<sup>10,11</sup> or bases such as KO<sup>t</sup>Bu along with stoichiometric amounts of hydride reagents (e.g., Et<sub>3</sub>SiH, alkali-metal based hydrides). In addition, such reactions also require high temperatures and pressures.<sup>12,13</sup>

As a result, extensive efforts have been dedicated to the development of catalytic methods, allowing the activation of ethers using H<sub>2</sub>.<sup>14–26</sup> For example, Hartwig and co-workers reported the selective activation of the C<sub>aryl</sub>–O bond of ethers under mild conditions (1 bar H<sub>2</sub>) using nickel catalysts.<sup>15,16</sup> The lanthanide triflates-catalyzed hydrogenolysis of ethers was reported by Marks and co-workers in which the in situ formed alkenols were hydrogenated using palladium nanoparticles to

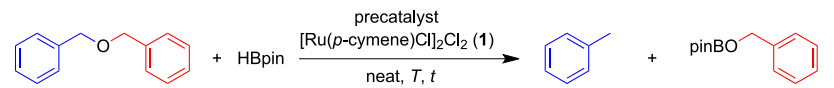
offset the thermodynamic barriers.<sup>17–19,21,22</sup> Similar to C–O bond activation, Chatani and co-workers reported the nickel-catalyzed C–N bond activation using HBpin under mild conditions.<sup>27</sup> While hydrogenolysis remains by far the most investigated method to cleave ether bonds, the development of alternative approaches recently gained increasing attention. In particular, Martin and co-workers reported the *ipso*-borylation of aryl methyl ethers via C–OMe bond cleavage.<sup>28</sup> This transformation involved a complex reaction medium containing a nickel catalyst, B<sub>2</sub>(nep)<sub>2</sub>, a base, a phosphine, and a solvent, and was limited to only a few substrates.<sup>28</sup> Recently, Okuda and co-workers developed an aluminum-based catalyst able to achieve the ring-opening of cyclic ethers (tetrahydrofuran and tetrahydropyran) through C–O bond cleavage via hydroboration.<sup>29–31</sup>

In this context, we show here that [Ru(*p*-cymene)Cl]<sub>2</sub>Cl<sub>2</sub> (**1**) acts as an efficient precatalyst for hydroboronolysis of a wide range of alkyl aryl ethers to the corresponding boronate esters and alkanes. The nature of the active species was

Received: October 1, 2020

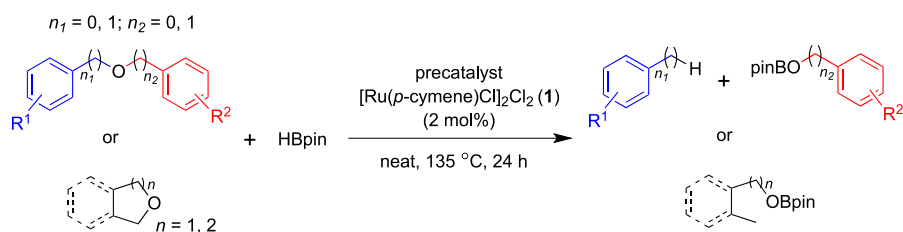
Revised: November 10, 2020



Table 1. Reaction Optimization for Hydroboronolysis of Dibenzylether<sup>a</sup>


entry	temp. (°C)	cat. (mol %)	time (h)	conv. (%)	PhCH <sub>2</sub> OBpin (%)
1	80	2	24	2	2
2	100	2	24	26	26
3	120	2	24	78	78
4	135	2	24	98	98
5	135	0.5	24	12	12
6	135	1	24	78	78
7	135	-	24	7	7

<sup>a</sup>Reaction conditions: dibenzylether (1 mmol), HBpin (2 mmol), and [Ru(*p*-cymene)Cl]<sub>2</sub>Cl<sub>2</sub> (1) (0.5–2.0 mol %) were heated in a closed vessel for 24 h (P<sub>atm</sub> at r.t., ca. 1.5 bar at 135 °C). Conversion of dibenzylether and yield of boronate ester were calculated using <sup>1</sup>H NMR.

Table 2. Catalytic Selective Hydroboronolysis of Dibenzyl Ethers and Arylbenzyl Ethers<sup>a</sup>

Entry	Ether	Conv. (%)	RH	ROBpin	Yield (ROBpin) (%) <sup>b</sup>
1		98			98
2		86			86
3		41			41
4		80			n.d.
5		47			47
6		87			69
7		74			64
8		96			96
9		84 (86)			n.d.
10		>99 (>99)			>99
11		>99 (>99)			83
12		90			84
13		21	-		21
14		0	-		0
15		64	-		64
16		58	-		58
17		-	-	-	n.d.

<sup>a</sup>Reaction conditions: ether (1 mmol), HBpin (2 mmol), and [Ru(*p*-cymene)Cl]<sub>2</sub>Cl<sub>2</sub> (1) (2 mol %) were heated at 135 °C in a closed vessel for 24 h (P<sub>atm</sub> at r.t., ca. 1.5 bar at 135 °C). Conversion of ethers was calculated using <sup>1</sup>H NMR; conversion calculated by GC is given in parentheses.

<sup>b</sup>Calculated based on <sup>1</sup>H NMR analysis of the reaction mixture. n.d.: not determined.

Table 3. Catalytic Selective Hydroboronolysis of Aliphatic Ethers<sup>a</sup>

$$\text{R}^1\text{-O-R}^2 + \text{HBpin} \xrightarrow[\text{neat, 135 }^\circ\text{C, 24 h}]{\text{precatalyst } [\text{Ru}(p\text{-cymene})\text{Cl}]_2\text{Cl}_2 \text{ (1) (2 mol\%)}}$$

$$\text{R}^1\text{H} + \text{pinBO-R}^2$$

Entry	Ether	Conv. (%)	RH	ROBpin	Yield (ROBpin) (%) <sup>b</sup>
1		>99	(40%) CH <sub>4</sub>	+	- 45
2		81			81
3		55			55
4		55			55
5		75			75
6		40	+	+	27 8
7		56	+	+	45 11
8		94 (95)	+	+	81 13
9		73			73
10		>99			>99
11		99			99
12		72			72
13		66			66
14		99	-	-	-

<sup>a</sup>Reaction conditions: ether (1 mmol), HBpin (2 mmol), and [Ru(*p*-cymene)Cl]<sub>2</sub>Cl<sub>2</sub> (**1**, 2 mol %) were heated at 135 °C in a closed vessel for 24 h (P<sub>atm</sub> at r.t., ca. 1.5 bar at 135 °C). Conversion of ethers was calculated using <sup>1</sup>H NMR; Conversion calculated by GC is given in parentheses.

<sup>b</sup>Calculated based on <sup>1</sup>H NMR analysis of the reaction mixture.

investigated using a combination of control experiments and characterization techniques, including NMR spectroscopy (in situ reaction monitoring), kinetics, poisoning experiments, and electron microscopy. The [Ru(*p*-cymene)Cl]<sub>2</sub>Cl<sub>2</sub> complex was converted into a mono-hydridobridged dinuclear species under the reaction conditions used, in agreement with previous observations.<sup>32–37</sup> The resulting [{(η<sup>6</sup>-*p*-cymene)RuCl]<sub>2</sub>(μ-H-μ-Cl)] (**2**) complex possesses high activity for hydroboronolysis of a wide range of ethers with various substituents in solvent-free conditions. The complex decomposes with time, forming Ru nanoparticles, which are moderately active for this transformation by a reduced factor of ca.15-fold. The catalytic system described provides an alternative approach for the cleavage of ethers, operates through both homogeneous and heterogeneous pathways, and may have possible application in biomass valorization.

## RESULTS AND DISCUSSION

Dibenzylether was selected as a model substrate and reacted with pinacolborane (HBpin = 4,4,5,5-tetramethyl-1,3,2-dioxaborolane) in the presence of the commercial [Ru(*p*-cymene)Cl]<sub>2</sub>Cl<sub>2</sub> complex (**1**). After a parameter screening, the best reaction conditions were found employing substrate (1 mmol), HBpin (2 mmol), **1** (2 mol %), 135 °C, and 24 h reaction time under neat conditions (Table 1, Entry 4). The pressure remains in all cases very close to atmospheric pressure (ca. 1.5 bar at 135 °C). Using these parameters, the reaction resulted in a 98% yield of benzyl boronate ester and toluene (Table 1, Entry 4). In general, lowering the temperature (Table 1, Entries 1–3) or decreasing the catalyst loading (Table 1, Entries 5, 6) provided reduced conversions and yields. Control experiments performed without the catalyst resulted in only very low conversion (7%, Table 1, Entry 7).

Table 4. Catalytic Selective Hydroboronolysis of Methylalkyl Ethers<sup>a</sup>

$$\text{R}^1\text{O}-\text{C}_n\text{H}_{2n+1} + \text{HBpin} \xrightarrow[\text{neat, 135 } ^\circ\text{C, 36 h}]{\text{precatalyst } [\text{Ru}(p\text{-cymene})\text{Cl}]_2\text{Cl}_2 \text{ (1) (5 mol\%)}} \text{CH}_4 + \text{pinBO}-\text{R}^1$$

Entry	Ether	Conv. (%)	RH		ROBpin	Yield (ROBpin) (%) <sup>b</sup>
1		>99	CH <sub>4</sub>	+		>99
2		78	CH <sub>4</sub>	+		78
3		74	CH <sub>4</sub>	+		74
4		78	CH <sub>4</sub>	+		78
5		92	CH <sub>4</sub>	+		92

<sup>a</sup>Reaction conditions: ether (1 mmol), HBpin (2 mmol), and [Ru(*p*-cymene)Cl]<sub>2</sub>Cl<sub>2</sub> (1, 5 mol %) were heated at 135 °C in a closed vessel for 36 h (P<sub>atm</sub> at r.t., ca. 1.5 bar at 135 °C). Conversion of ethers was calculated using <sup>1</sup>H NMR. <sup>b</sup>Calculated based on <sup>1</sup>H NMR analysis of reaction mixture.

Using the optimized conditions, hydroboronolysis of various dibenzyl ethers and arylbenzyl ethers was explored (Table 2). Symmetrical substrates were all converted into their corresponding products in moderate to excellent yields (40–98%, Entries 1–6). A particular focus was placed on unsymmetrical substrates to understand the influence of substituents on the selectivity. Using unsymmetrical dibenzyl ethers (Entries 7 and 8), the cleavage occurred preferentially on the relatively electron-poor C–O bond, producing 4-methylbenzylpinacol boronate ester and 4-*tert*-butylbenzyl boronate ester in high selectivity. Considering unsymmetrical arylbenzyl ethers as substrates (Entries 9–12), the corresponding arylboronate esters were obtained in good to excellent yields (80–99%). Selective hydroboronolysis of the C<sub>Bn</sub>–O bond (Bn = benzyl) in this case is attributed to the stronger bond strength of the aryl–C–O bond. To confirm this hypothesis, DFT calculation was performed for hydroboronolysis of (benzyloxy)benzene (Table 2, Entry 9). The results from DFT calculation affirmed that the dissociation energy of the aryl–C–O bond (82.45 ± 5 kcal·mol<sup>−1</sup>) is higher than that of the C<sub>Bn</sub>–O bond (BDE = 38.74 ± 5 kcal·mol<sup>−1</sup>) and the reaction favors the formation of thermodynamically controlled products (see Supporting Information, Table S1).

The scope of cyclic ethers was also explored. The reaction of tetrahydropyran with HBpin confirmed the formation of 4,4,5,5-tetramethyl-2-(pentyloxy)-1,3,2-dioxaborolane with a moderate yield of 21% but excellent selectivity (Entry 13). Hydroboronolysis of tetrahydrofuran was not observed under these conditions (Entry 14). Phthalan and isochromane provided the corresponding ring-opening products 4,4,5,5-tetramethyl-2-((2-methylbenzyl)oxy)-1,3,2-dioxaborolane and 4,4,5,5-tetramethyl-2-(2-methylphenethoxy)-1,3,2-dioxaborolane, in moderate yields (64 and 58%, respectively; Entries 15 and 16). When a heterocyclic ether such as 2-((benzyloxy)methyl)pyridine was subjected to hydroboronolysis, the formation of a complex product mixture was observed (Entry 17).

To investigate the versatility of the precatalyst 1 for hydroboronolysis, more challenging substrates were considered, that is, ethers containing various alkyl and benzyl substituents (Table 3). When benzylmethyl ether was used as the substrate,

toluene (40%) and benzylboronate ester (45%) were formed, indicating a competing cleavage between the C<sub>Bn</sub>–O and C<sub>methyl</sub>–O bonds (Entry 1). ((Heptyloxy)methyl)benzene was converted into heptylboronate ester in high yield (81%), evidencing an excellent selectivity toward the cleavage of the C<sub>Bn</sub>–O bond (Entry 2). Similar observations were made using sterically hindered alkyl benzyl ethers, with somewhat lower yields (Entries 3–5). With the introduction of electron-donating substituents on the para position of the phenyl ring, a partial C<sub>alkyl</sub>–O bond cleavage was observed (8–11%), while C<sub>Bn</sub>–O bond cleavage remained predominant (Entries 6 and 7). (2-(Benzyloxy)ethyl)benzene was almost fully converted (94%) to provide the 81% C<sub>Bn</sub>–O activation product, while C<sub>phenethyl</sub>–O bond breaking yielded the corresponding boronate ester in 13% yield (Entry 8). The C<sub>Bn</sub>–O bond was selectively cleaved in (4-(benzyloxy)butyl)benzene, providing the corresponding 4-phenylbutyl boronate ester in 73% yield (Entry 9). Various alkyl chain tethered bis(benzyl) diether derivatives were also considered. In all cases, the cleavage occurred selectively on C<sub>Bn</sub>–O bonds and the corresponding dialkylboronate esters were obtained in moderate to near quantitative yields (Entries 10–13). However, when a sterically hindered ether such as (oxybis(ethane-1,1-diyl))dibenzene was used as the substrate, complete consumption of the ether occurred and resulted in the formation of unidentified products, perhaps due to the sensitivity of secondary benzylic carbocation (Entry 14).

Then, the more challenging deconstruction of the C<sub>Me</sub>–O bond in alkylmethyl ethers was investigated (Table 4). (4-Methoxybutyl)benzene was initially subjected to 2 mol % of the ruthenium precatalyst 1, resulting in only 42% conversion. Under similar conditions, 1-methoxydecane and 1,8-dimethoxyoctane reached conversions of 25 and 23%, respectively. To enhance the substrate conversion and product yield, 5 mol % of the precatalyst 1 and longer reaction time (36 h) were used for hydroboronolysis of alkylmethyl ethers. Using these adapted conditions, (2-methoxyethyl)benzene was quantitatively converted into 2-phenethyloxy boronate ester and methane (Entry 1). Under similar conditions, various methyl ethers such as (4-methoxybutyl)benzene, 1-methoxydecane, 1,8-dimethoxyoctane, and 1,10-dimethoxydecane were used as substrates,

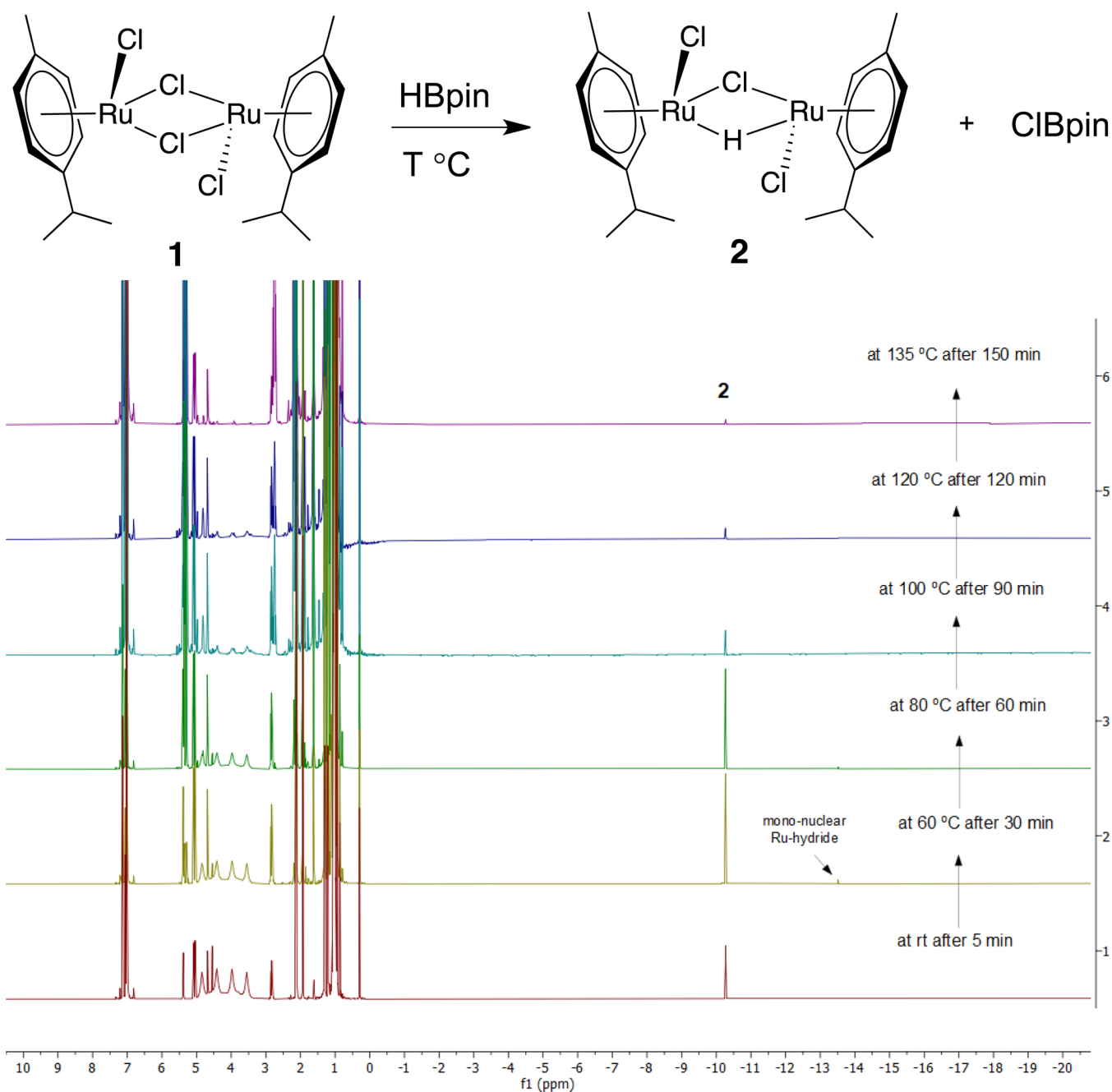


**Figure 1.** Reaction of HBpin with Ru-precatalyst **1**. Reaction conditions:  $[\text{Ru}(p\text{-cymene})\text{Cl}]_2\text{Cl}_2$  (**1**) (0.01 mmol), HBpin (0.022 mmol) and  $\text{tol-d}^8$  (0.5 mL) were heated at indicated reaction temperature,  $^1\text{H}$  NMR (400 MHz,  $\text{tol-d}^8$ ,  $T$ ).

providing their corresponding boronate and diboronate esters in 74 to 92% yields (Entries 2–5). Notably, excellent selectivity was observed for all these substrates. Sanford and Mindiola independently reported selective C–H borylation of methane under pressurized conditions.<sup>38,39</sup> Under our experimental condition, no C–H borylation was observed.

**Mechanistic Studies: Evidence for the Form of the Ru-Based Catalyst.** The efficiency and versatility of the precatalyst **1** has now been demonstrated, but the exact nature of the active species is not obvious. In particular, we have previously shown that the use of complex **1** in the presence of HBpin results in the immediate formation of a dinuclear monohydrido bridged ruthenium complex  $[\{(\eta^6\text{-}p\text{-cymene})\text{-RuCl}\}_2(\mu\text{-H}-\mu\text{-Cl})]$  (**2**).<sup>32–35</sup> Since the hydroboration activity

was observed at 120 °C and above [see Table 1, Entry 3], the in situ formation of **2** from the reaction of **1** with HBpin was envisaged. To investigate this hypothesis, in situ monitoring by  $^1\text{H}$  NMR of a stoichiometric reaction between **1** and HBpin was performed at different temperatures, confirming the very quick formation of complex **2** (apparition of a sharp singlet at  $\delta = -10.26$  ppm in  $^1\text{H}$  NMR characteristic of the “bridged hydride” in **2**) under the reaction conditions used (Figure 1 and Figures S1,S2). Complex **2** was found stable up to ca. 100 °C, but started decomposing above that temperature, presumably reduced by HBpin or  $\text{H}_2$  elimination to form ruthenium nanoparticles. At 135 °C, the signal associated with complex **2** disappeared after ca. 50 min (Figure S2). A comparable in situ NMR monitoring performed in the

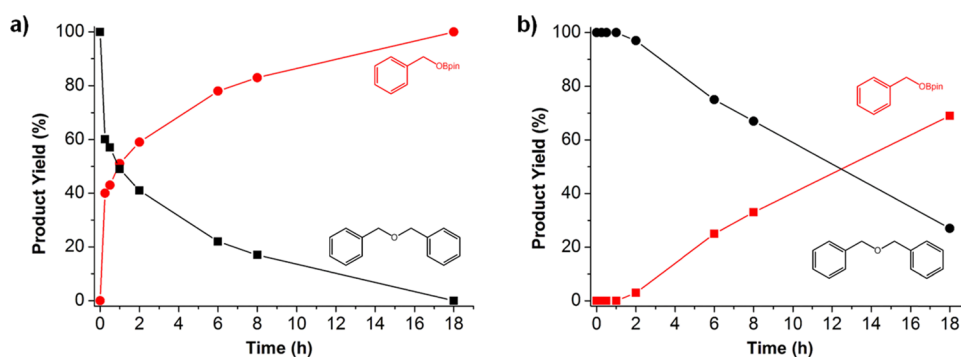


**Figure 2.** Time profiles for the conversion of dibenzylether to benzylboronate ester and toluene. (a) Without poison. (b) With 2 equiv. DCT (dibenzo[*a,e*]cyclooctatetraene) as poison. Reaction conditions: dibenzylether (1 mmol), HBpin (2 mmol), and [Ru(*p*-cymene)Cl]<sub>2</sub>Cl<sub>2</sub> (1, 2 mol %) at 135 °C.

presence of dibenzyl ether also led to similar observations (see Supporting Information, Figures S3–S6). In addition, in situ formed mononuclear Ru–H species were previously found to play a crucial role in the hydroelementation reactions of unsaturated organic functionalities.<sup>32–35</sup> The formation of such Ru–H species was observed in <sup>1</sup>H NMR analysis ( $\delta = -13.6$  ppm, Figure 1) of reaction mixtures up to 80 °C and found to decompose at higher temperatures (Figure 1 and Figures S4,S6). As hydroboronolysis of ethers is observed above 120 °C, this is some evidence that mononuclear Ru–H species are not involved in catalysis. In addition, the reaction performed at 135 °C in the absence of HBpin and only with dibenzyl ether failed to produce any black precipitate and nanoparticles. The resulting reaction mixture consisted of a homogeneous red solution, indicating that the decomposition/reduction of complex **2** indeed requires the presence of HBpin.

In addition, the solution after catalysis is black, suggesting the decomposition of the Ru complex **2** to form clusters or nanoparticles. Very recently, we investigated the hydrogenation of heteroarenes and arenes employing complex **2**. The outcome from this study revealed that the hydrogenation of heteroarenes proceeds via homogeneous catalysis and arenes hydrogenation via heterogeneous catalysis, confirming that dual catalysis is accessible starting from complex **2**.<sup>40</sup> To determine whether the hydroboronolysis activity observed is due to a homogeneous or heterogeneous catalyst, we started by investigating the kinetics of the reaction using dibenzylether as a model substrate. For that, a time profile was recorded under the optimized conditions (Figure 2a). The profile shows a very quick formation of benzylboronate ester (and toluene) in the first 30 min (45% yield after 30 min), followed by a slow and progressive increase of the yield to reach 100% after 18 h. This indicates that active species are present in the reaction mixture from the beginning. A second time profile was recorded, but this time in the presence of two equivalents of DCT (dibenzo[*a,e*]cyclooctatetraene), known to be a very efficient poison for molecular catalysts (Figure 2b).<sup>41</sup> The profile is, in this case, completely different, with no product formation in the first hour, followed by a slow and progressive increase of the product yield in the next hours. These results are consistent with a molecular complex being responsible for the high activity in the initial times of the reaction. A molecular catalyst is consistent with the kinetic data from Figures S2,S6, which show that complex **2** is present in the reaction mixture during the first 30–60 min. Then, after an induction period of

ca. 2 h, some product formation was observed, evidencing the presence of a heterogeneous catalyst.

Altogether, these observations are consistent with complex **2** being highly active for hydroboronolysis and responsible for the very high reaction rate in the first 30 min (initial rate  $k = 0.90$  mmol·h<sup>-1</sup>). After that, complex **2** is completely decomposed to form Ru nanoparticles, which are also catalyzing this transformation but with an apparent lower activity (initial rate  $k' = 0.06$  mmol·h<sup>-1</sup>, meaning that **2** is ca. 15-fold more active than the Ru NPs formed in situ). Interestingly, the slope of product formation after 2 h is very similar in both cases (with and without poison), strongly suggesting that after 2 h, Ru NPs are the only species responsible for the activity observed. TEM and EDX analyses were performed on the black material collected after catalysis to confirm the formation of small Ru nanoparticles (Figure 3 and see Supporting Information, Figure S8).

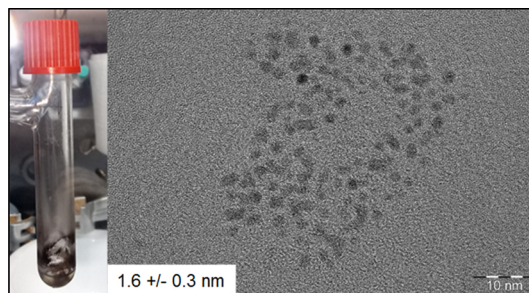


**Figure 3.** Characterization of the material obtained after catalysis. Left: picture of the Schlenk tube after catalysis, showing a black precipitate. Right: TEM analysis of the black precipitate.

Using the collected nanoparticles directly as catalysts for hydroboronolysis of dibenzyl ether, 78% yield of benzylboronate ester was obtained after 24 h. Additional poisoning experiment on the recycled catalyst using mercury (50 mol %) resulted in low conversion (18%) after 24 h, further supporting the involvement of Ru NPs. Importantly, performing the reaction without any precatalyst **1** results in a product yield of 7% (Table 1, Entry 7) after 24 h. 1,10-Phenanthroline was previously shown to be a very good poison for Rh and Ru NPs in hydrogenation reactions at 100 °C, allowing the differentiation between clusters and NPs when performing quantitative poisoning experiments.<sup>42–44</sup> Interestingly, its use was not successful in this particular case. The addition of 1,10-phenanthroline to catalytic hydroboronolysis involving the

recycled catalyst did not significantly affect the activity, even in large excess (Figure S7). In this particular case, this can be due to a combination of the neat substrate conditions and maybe also the somewhat higher temperature (135 °C here vs 100 °C in the literature<sup>15</sup>) that favor reversal of the exothermic binding of 1,10-phenanthroline.<sup>42–44</sup> This suggests that 1,10-phenanthroline is not able to efficiently poison Ru NPs for this particular transformation under these conditions. In addition, preparing Ru nanoparticles on purpose in an ionic liquid<sup>45</sup> and using them as catalysts resulted as well in the production of benzylboronate ester (52%), confirming that Ru NPs are active in hydroboronolysis.

## CONCLUSIONS

In summary, the first such report of catalytic hydroboronolysis of ethers is described. Complex **1** is employed as simple precatalyst, and the reactions are conducted under neat conditions. In unsymmetrical ethers, hydroboronolysis occurs selectively on electron-poor C–O bonds; thus, C<sub>Bn</sub>–OR (R = aryl or alkyl) bonds are selectively activated in arylbenzyl and alkylbenzyl ethers to provide the corresponding boronate esters and aryl alkanes. In alkylmethyl ethers, C<sub>Me</sub>–OR bonds are activated. The cleavage of ethers is also applicable to cyclic and other aliphatic ether compounds. Mechanistic studies involving <sup>1</sup>H NMR, time profile, quantitative poisoning indicated the immediate formation of intermediate complex **2** from the precatalyst **1** in the presence of HBpin. In addition, the in situ generation of Ru NPs from **2** was confirmed by electron microscopy. Complex **2** is implicated as a highly active catalyst for hydroboronolysis at the initial stage of the reactions. However, over time, **2** decomposes and produces Ru NPs, which also catalyze the hydroboronolysis activity albeit at an apparent slower rate. The presented results highlight the substantial scope of hydroboronolysis as a useful transformation in organic synthesis and as an alternative approach to hydrogenolysis. Applications including the deconstruction of ether linkages in lignocellulosic biomass using this protocol can be anticipated.

## ASSOCIATED CONTENT

### Supporting Information

The Supporting Information is available free of charge at <https://pubs.acs.org/doi/10.1021/acscatal.0c04269>.

Experimental procedures, spectral data, details of mechanistic studies, and copies of <sup>1</sup>H, <sup>13</sup>C NMR spectra of the products. (PDF)

## AUTHOR INFORMATION

### Corresponding Author

**Chidambaram Gunanathan** – School of Chemical Sciences, National Institute of Science Education and Research (NISER), HBNI, Bhubaneswar 752050, India; [orcid.org/0000-0002-9458-5198](https://orcid.org/0000-0002-9458-5198); Email: [gunanathan@niser.ac.in](mailto:gunanathan@niser.ac.in)

### Authors

**Akash Kaithal** – School of Chemical Sciences, National Institute of Science Education and Research (NISER), HBNI, Bhubaneswar 752050, India; Max Planck Institute for Chemical Energy Conversion, 45470 Mülheim an der Ruhr, Germany

**Deepti Kalsi** – Max Planck Institute for Chemical Energy Conversion, 45470 Mülheim an der Ruhr, Germany

**Varadhan Krishnakumar** – School of Chemical Sciences, National Institute of Science Education and Research (NISER), HBNI, Bhubaneswar 752050, India; [orcid.org/0000-0001-9400-3429](https://orcid.org/0000-0001-9400-3429)

**Sandip Pattanaik** – School of Chemical Sciences, National Institute of Science Education and Research (NISER), HBNI, Bhubaneswar 752050, India

**Alexis Bordet** – Max Planck Institute for Chemical Energy Conversion, 45470 Mülheim an der Ruhr, Germany; [orcid.org/0000-0003-0133-3416](https://orcid.org/0000-0003-0133-3416)

**Walter Leitner** – Max Planck Institute for Chemical Energy Conversion, 45470 Mülheim an der Ruhr, Germany; Institut für Technische und Makromolekulare Chemie, RWTH Aachen University, 52074 Aachen, Germany; [orcid.org/0000-0001-6100-9656](https://orcid.org/0000-0001-6100-9656)

Complete contact information is available at:

<https://pubs.acs.org/10.1021/acscatal.0c04269>

## Notes

The authors declare no competing financial interest.

## ACKNOWLEDGMENTS

The authors thank SERB New Delhi (EMR/2016/002517), Department of Atomic Energy, India, and NISER for financial support, and Dr. P. S. Subramanian for his kind help. V.K. thanks SERB for the National Postdoctoral Fellowship. S.P. thanks CSIR for a Fellowship. The authors also acknowledge the financial support by the Max Planck Society and by the Deutsche Forschungsgemeinschaft (DFG, German Research Foundation) under Germany's Excellence Strategy – Exzellenzcluster 2186 “The Fuel Science Center” ID: 390919832. Furthermore, the authors would like to thank Norbert Pfänder (MPI for Chemical Energy Conversion, Mülheim an der Ruhr), Adrian Schlüter (MPI for Kohlenforschung, Mülheim an der Ruhr) for electron microscopy characterization.

## DEDICATION

Dedicated to Prof. S. Chandrasekaran on the occasion of his 75th birthday.

## REFERENCES

- Ragauskas, A. J.; Beckham, G. T.; Biddy, M. J.; Chandra, R.; Chen, F.; Davis, M. F.; Davison, B. H.; Dixon, R. A.; Gilna, P.; Keller, M.; Langan, P.; Naskar, A. K.; Saddler, J. N.; Tschaplinski, T. J.; Tuskan, G. A.; Wyman, C. E. Lignin Valorization: Improving Lignin Processing in the Biorefinery. *Science* **2014**, *344*, 709–719.
- Xu, C.; Arancon, R. A. D.; Labidi, J.; Luque, R. Lignin depolymerisation strategies: towards valuable chemicals and fuels. *Chem. Soc. Rev.* **2014**, *43*, 7485–7500.
- Li, C.; Zhao, X.; Wang, A.; Huber, G. W.; Zhang, T. Catalytic Transformation of Lignin for the Production of Chemicals and Fuels. *Chem. Rev.* **2015**, *115*, 11559–11624.
- Huber, G. W.; Iborra, S.; Corma, A. Synthesis of Transportation Fuels from Biomass: Chemistry, Catalysts, and Engineering. *Chem. Rev.* **2006**, *106*, 4044–4098.
- Zakzeski, J.; Bruijninx, P. C. A.; Jongerius, A. L.; Weckhuysen, B. M. The Catalytic Valorization of Lignin for the Production of Renewable Chemicals. *Chem. Rev.* **2010**, *110*, 3552–3599.
- Azadi, P.; Inderwildi, O. R.; Farnood, R.; King, D. A. Liquid fuels, hydrogen and chemicals from lignin: A critical review. *Renew. Sustain. Energy Rev.* **2013**, *21*, 506–523.

- (7) Rahimi, A.; Ulbrich, A.; Coon, J. J.; Stahl, S. S. Formic-acid-induced depolymerization of oxidized lignin to aromatics. *Nature* **2014**, *515*, 249–252.
- (8) Zaheer, M.; Kempe, R. Catalytic Hydrogenolysis of Aryl Ethers: A Key Step in Lignin Valorization to Valuable Chemicals. *ACS Catal.* **2015**, *5*, 1675–1684.
- (9) Hartung, W. H.; Simonoff, R. Hydrogenolysis of Benzyl Groups Attached to Oxygen, Nitrogen, or Sulfur. *Org. React.* **2004**, *7*, 263–326.
- (10) Burwell, R. L. The Cleavage of Ethers. *Chem. Rev.* **1954**, *54*, 615–685.
- (11) Jung, M. E.; Lyster, M. A. Cleavage of Methyl Ethers with Iodotrimethylsilane: Cyclohexanol from Cyclohexyl Methyl Ether. *Org. Synth.* **2003**, *59*, 35.
- (12) Fedorov, A.; Toutov, A. A.; Swisher, N. A.; Grubbs, R. H. Lewis-base silane activation: from reductive cleavage of aryl ethers to selective ortho-silylation. *Chem. Sci.* **2013**, *4*, 1640–1645.
- (13) Xu, H.; Liu, X.; Zhao, Y.; Wu, C.; Chen, Y.; Gao, X.; Liu, Z. Reductive Cleavage of C–O Bond in Model Compounds of Lignin. *Chin. J. Chem.* **2017**, *35*, 938–942.
- (14) Nichols, J. M.; Bishop, L. M.; Bergman, R. G.; Ellman, J. A. Catalytic C–O Bond Cleavage of 2-Aryloxy-1-arylethanol and Its Application to the Depolymerization of Lignin-Related Polymers. *J. Am. Chem. Soc.* **2010**, *132*, 12554–12555.
- (15) Sergeev, A. G.; Hartwig, J. F. Selective, Nickel-Catalyzed Hydrogenolysis of Aryl Ethers. *Science* **2011**, *332*, 439–443.
- (16) Sergeev, A. G.; Webb, J. D.; Hartwig, J. F. A Heterogeneous Nickel Catalyst for the Hydrogenolysis of Aryl Ethers without Arene Hydrogenation. *J. Am. Chem. Soc.* **2012**, *134*, 20226–20229.
- (17) Atesin, A. C.; Ray, N. A.; Stair, P. C.; Marks, T. J. Etheric C–O Bond Hydrogenolysis Using a Tandem Lanthanide Triflate/Supported Palladium Nanoparticle Catalyst System. *J. Am. Chem. Soc.* **2012**, *134*, 14682–14685.
- (18) Assary, R. S.; Atesin, A. C.; Li, Z.; Curtiss, L. A.; Marks, T. J. Reaction Pathways and Energetics of Etheric C–O Bond Cleavage Catalyzed by Lanthanide Triflates. *ACS Catal.* **2013**, *3*, 1908–1914.
- (19) Li, Z.; Assary, R. S.; Atesin, A. C.; Curtiss, L. A.; Marks, T. J. Rapid Ether and Alcohol C–O Bond Hydrogenolysis Catalyzed by Tandem High-Valent Metal Triflate + Supported Pd Catalysts. *J. Am. Chem. Soc.* **2013**, *136*, 104–107.
- (20) Haibach, M. C.; Lease, N.; Goldman, A. S. Catalytic Cleavage of Ether C–O Bonds by Pincer Iridium Complexes. *Angew. Chem., Int. Ed.* **2014**, *53*, 10160–10163.
- (21) Lohr, T. L.; Li, Z.; Marks, T. J. Selective Ether/Ester C–O Cleavage of an Acetylated Lignin Model via Tandem Catalysis. *ACS Catal.* **2015**, *5*, 7004–7007.
- (22) Lohr, T. L.; Li, Z.; Marks, T. J. Thermodynamic Strategies for C–O Bond Formation and Cleavage via Tandem Catalysis. *Acc. Chem. Res.* **2016**, *49*, 824–834.
- (23) Cui, X.; Yuan, H.; Junge, K.; Topf, C.; Beller, M.; Shi, F. A stable and practical nickel catalyst for the hydrogenolysis of C–O bonds. *Green Chem.* **2017**, *19*, 305–310.
- (24) Bulut, S.; Siankevich, S.; van Muyden, A. P.; Alexander, D. T. L.; Savoglidis, G.; Zhang, J.; Hatzimanikatis, V.; Yan, N.; Dyson, P. J. Efficient cleavage of aryl ether C–O linkages by Rh–Ni and Ru–Ni nanoscale catalysts operating in water. *Chem. Sci.* **2018**, *9*, 5530–5535.
- (25) Li, J.; Sun, H.; Liu, J.-X.; Zhang, J.-J.; Li, Z.-X.; Fu, Y. Selective reductive cleavage of CO bond in lignin model compounds over nitrogen-doped carbon-supported iron catalysts. *Mol. Catal.* **2018**, *452*, 36–45.
- (26) Rengshausen, S.; Etscheidt, F.; Großkurth, J.; Luska, K. L.; Bordet, A.; Leitner, W. Catalytic Hydrogenolysis of Substituted Diaryl Ethers by Using Ruthenium Nanoparticles on an Acidic Supported Ionic Liquid Phase (Ru@SILP-SO<sub>3</sub>H). *Synlett* **2019**, *30*, 405–412.
- (27) Tobisu, M.; Nakamura, K.; Chatani, N. Nickel-Catalyzed Reductive and Borylative Cleavage of Aromatic Carbon–Nitrogen Bonds in *N*-Aryl Amides and Carbamates. *J. Am. Chem. Soc.* **2014**, *136*, 5587–5590.
- (28) Zarate, C.; Manzano, R.; Martin, R. Ipso-Borylation of Aryl Ethers via Ni-Catalyzed C–OMe Cleavage. *J. Am. Chem. Soc.* **2015**, *137*, 6754–6757.
- (29) Mukherjee, D.; Osseili, H.; Truong, K.-N.; Spaniol, T. P.; Okuda, J. Ring-opening of cyclic ethers by aluminum hydridotriphenylborate. *Chem. Commun.* **2017**, *53*, 3493–3496.
- (30) Lampland, N. L.; Hovey, M.; Mukherjee, D.; Sadow, A. D. Magnesium-Catalyzed Mild Reduction of Tertiary and Secondary Amides to Amines. *ACS Catal.* **2015**, *5*, 4219–4226.
- (31) Yang, Y.; Anker, M. D.; Fang, J.; Mahon, M. F.; Maron, L.; Weetman, C.; Hill, M. S. Hydrodeoxygenation of isocyanates: snapshots of a magnesium-mediated C–O bond cleavage. *Chem. Sci.* **2017**, *8*, 3529–3537.
- (32) Kaithal, A.; Chatterjee, B.; Gunanathan, C. Ruthenium Catalyzed Selective Hydroboration of Carbonyl Compounds. *Org. Lett.* **2015**, *17*, 4790–4793.
- (33) Kaithal, A.; Chatterjee, B.; Gunanathan, C. Ruthenium-Catalyzed Selective Hydroboration of Nitriles and Imines. *J. Org. Chem.* **2016**, *81*, 11153–11161.
- (34) Kisan, S.; Krishnakumar, V.; Gunanathan, C. Ruthenium-Catalyzed Anti-Markovnikov Selective Hydroboration of Olefins. *ACS Catal.* **2017**, *7*, 5950–5954.
- (35) Chatterjee, B.; Gunanathan, C. Ruthenium catalyzed selective hydrosilylation of aldehydes. *Chem. Commun.* **2014**, *50*, 888–890.
- (36) Bennett, M. A.; Ennett, J. P. Synthesis and spectroscopic characterization of dinuclear mono( $\mu$ -hydrido)arene complexes of divalent ruthenium. *Organometallics* **1984**, *3*, 1365–1374.
- (37) Süß-Fink, G.; Garcia Fidalgo, E.; Neels, A.; Stoeckli-Evans, H. Reactivity of dinuclear arene ruthenium complexes: reactions of the hydrido complex [(*p*-Me-C<sub>6</sub>H<sub>4</sub>-Pr<sup>i</sup>)<sub>2</sub>Ru<sub>2</sub>Cl<sub>2</sub>( $\mu$ -Cl)( $\mu$ -H)] with NaX and HX (X=F, Cl, Br, I). *J. Organomet. Chem.* **2000**, *602*, 188–192.
- (38) Cook, A. K.; Schimmler, S. D.; Matzger, A. J.; Sanford, M. S. Catalyst-controlled selectivity in the C–H borylation of methane and ethane. *Science* **2016**, *351*, 1421–1424.
- (39) Smith, K. T.; Berritt, S.; González-Moreiras, M.; Ahn, S.; Smith, M. R.; Baik, M.-H.; Mindiola, D. J. Catalytic borylation of methane. *Science* **2016**, *351*, 1424–1427.
- (40) Chatterjee, B.; Kalsi, D.; Kaithal, A.; Bordet, A.; Leitner, W.; Gunanathan, C. One-pot dual catalysis for the hydrogenation of heteroarenes and arenes. *Catal. Sci. Technol.* **2020**, *10*, 5163–5170.
- (41) Anton, D. R.; Crabtree, R. H. Dibenzo[a,e]cyclooctatetraene in a proposed test for heterogeneity in catalysts formed from soluble platinum-group metal complexes. *Organometallics* **1983**, *2*, 855–859.
- (42) Widegren, J. A.; Finke, R. G. A review of the problem of distinguishing true homogeneous catalysis from soluble or other metal-particle heterogeneous catalysis under reducing conditions. *J. Mol. Catal. A: Chem.* **2003**, *198*, 317–341.
- (43) Bayram, E.; Linehan, J. C.; Fulton, J. L.; Roberts, J. A. S.; Szymczak, N. K.; Smurthwaite, T. D.; Özkar, S.; Balasubramanian, M.; Finke, R. G. Is It Homogeneous or Heterogeneous Catalysis Derived from [RhCp\*Cl<sub>2</sub>]<sub>2</sub>? In Operando XAFS, Kinetic, and Crucial Kinetic Poisoning Evidence for Subnanometer Rh<sub>4</sub> Cluster-Based Benzene Hydrogenation Catalysis. *J. Am. Chem. Soc.* **2011**, *133*, 18889–18902.
- (44) Bayram, E.; Finke, R. G. Quantitative 1,10-Phenanthroline Catalyst-Poisoning Kinetic Studies of Rh(0) Nanoparticle and Rh<sub>4</sub> Cluster Benzene Hydrogenation Catalysts: Estimates of the Poison  $K_{\text{association}}$  Binding Constants, of the Equivalents of Poison Bound and of the Number of Catalytically Active Sites for Each Catalyst. *ACS Catal.* **2012**, *2*, 1967–1975.
- (45) Julis, J.; Hölscher, M.; Leitner, W. Selective hydrogenation of biomass derived substrates using ionic liquid-stabilized ruthenium nanoparticles. *Green Chem.* **2010**, *12*, 1634–1639.